POLISH MARITIME RESEARCH 4 (120) 2023 Vol. 30; pp. 92-101
10.2478/pomr-2023-0062

AN EXPERIMENTAL STUDY OF THE EFFECTS OF CYLINDER LUBRICATING OILS ON THE VIBRATION CHARACTERISTICS OF A TWO-STROKE LOW-SPEED MARINE DIESEL ENGINE

Gang Wu [1*]
Guodong Jiang [1]
Changsheng Chen [2]
Guohe Jiang [1]
Xigang Pu [1]
Biwen Chen [2]
[1] Merchant Marine College, Shanghai Maritime University, Shanghai, China
[2] Shanghai Marine Equipment Research Institute, Shanghai, China

* Corresponding author: *wugang@shmtu.edu.cn (Gang Wu)*

ABSTRACT

Two-stroke, low-speed diesel engines are widely used in large ships due to their good performance and fuel economy. However, there have been few studies of the effects of lubricating oils on the vibration of two-stroke, low-speed diesel engines. In this work, the effects of three different lubricating oils on the vibration characteristics of a low-speed engine are investigated, using the frequency domain, time-frequency domain, fast Fourier transform (FFT) and short-time Fourier transform (STFT) methods. The results show that non-invasive condition monitoring of the wear to a cylinder liner in a low-speed marine engine can be successfully achieved based on vibration signals. Both the FFT and STFT methods are capable of capturing information about combustion in the cylinder online in real time, and the STFT method also provides the ability to visualise the results with more comprehensive information. From the online condition monitoring of vibration signals, cylinder lubricants with medium viscosity and medium alkali content are found to have the best wear protection properties. This result is consistent with those of an elemental analysis of cylinder lubrication properties and an analysis of the data measured from a piston lifted from the cylinder after 300 h of engine operation.

Keywords: two-stroke; low-speed marine diesel engine; cylinder lubricating oils; vibration characteristic; condition monitoring

INTRODUCTION

The internal combustion (IC) engine is a classical rotating power machine that has been widely employed for transportation and power production [1]. In particular, the two-stroke low-speed diesel engine is a unique type of IC engine that has been used in many medium and large ships due to its advantages such as multi-fuel feasibility, fuel economy, large output power, and durability [2]. With the increasing emphasis on ship safety, more and more researchers are focusing on the hazards to reliability posed by engine vibration. Harmful engine vibration can have direct effects on the hull, machinery, crew, and passengers when it occurs in ships. The main source of engine vibration is an imbalance in the force and moment created by the inertial force of its moving parts, although another source is the side thrust and overturning moment generated by the in-cylinder pressure of fuel combustion. Further factors include the influence of lubricating oils [3, 4], fuels [5-8], and engine faults [9, 10], which can all affect engine vibration. The engine contains many internal components, such as the piston-cylinder assembly, which require a good lubricating oil to run; hence, the characteristics of the lubricating oil, and its quality and

performance, will have a significant impact on the behaviour of the engine, especially for two-stroke low-speed marine diesel engines with complex structures and large dimensions.

In general, lubricating oil is an oil-like liquid that is applied between moving surfaces and can carry out the functions of reducing friction and wear. It also has the ability to eliminate shock loads, and can ensure cooling, sealing, etc. Thus, lubricating oil requires several properties, such as a suitable viscosity, flash point, and alkali value, which are related to the functions mentioned above. Prior research [11] has confirmed the importance of the properties of the lubricant, as it affects not only the engine itself but also attached components such as turbochargers, meaning that it is very important in terms of the transient response of the engine. The viscosity-temperature characteristics of lubricating oil reveal the relationship between viscosity and temperature, where the lower the temperature, the higher the viscosity. This relationship is strongly related to the performance of the engine, as a high viscosity for the lubricating oil will increase the friction loss of the engine, especially in a low-temperature environment. It is therefore important to develop suitable grades of engine lubricating oil with different viscosities. The American Society of Automotive Engineers (SAE) grading system is widely used internationally to represent the viscosity of lubricating oil.

Lubricating oil with different properties can produce different levels of friction and wear in an engine, which can lead to different vibration characteristics and different amounts of wear to metals from the lubricating oil used. In research conducted by Ahmad Taghizadeh-Alisaraei, it was found that the replacement of lubricating oil helps to reduce engine vibration, as it can reduce the friction between components such as bearings, piston cylinders, etc. [12]. One potential reason for this is that degradation of the lubricating oil and the presence of wear debris in the unreplaced lubricating oil lead to greater engine vibration. Recent studies have revealed further information on the effects of fuel type on the status of lubrication oil. Nantha Gopal et al. [13] studied the effects of biodiesel fuel on the surface wear to cylinder liners, and quantified the cylinder wear of the engine by comparing the surface roughness of the cylinder liner as well as the concentration of wear debris in the lubricant samples from the engine. The results revealed significant degradation of the lubricating oil in a biodiesel blended fuel engine. A further analysis of the oil revealed the presence of wear metals in the used oil, which were also considered to be related to degradation. Hence, the problem of degradation is critical for lubrication oil, as it can cause a significant reduction in the kinematic viscosity and the flash point of the lubricating oil.

For a two-stroke low-speed marine diesel engine, the type of lubrication required for the cylinder liner is unique. A larger cylinder bore and a longer cylinder stroke require a greater injection of lubricating oil to the cylinder. In addition, matching the sulphur level of heavy fuel oil (HFO) to the cylinder lubricating oil is a critical issue. This requires that the cylinder lubricating oil has an appropriate alkali value: if too little alkali is present, the acids in the combustion products will not be neutralised and will attack the piston liner, causing corrosive wear, whereas if too much alkali is present, inorganic calcium carbonate will form hard deposits that cannot be burned out, leading to abrasive wear. With the trend towards low-sulphur fuel, there is a lack of experience in terms how to address the issues of lubricity and cleanliness between the piston and cylinder liner. In addition, the traditional method of inspecting the piston and cylinder liner relies on manual disassembly of the piston-cylinder assembly, which is not efficient.

In recent years, vibration and noise signals have been shown to be useful for assessing the condition of engines, such as combustion processes, valve faults, and fuel injection behaviours, and can be used for fault detection in diesel engines. Researchers have already begun to investigate engine performance and optimal fuel selection based on engine vibration signals. Ahmad Taghizadeh-Alisaraei [12] designed a systematic experiment to evaluate the minimum engine vibration for seven engine speeds and nine biodiesel fuel blend ratios by calculating the root mean square (RMS) and comparing the amplitudes of the vibration signals. Ahmet Çalık [14] measured the vibration characteristics of an engine when hydrogen was added to biodiesel. The RMS was used to compare the vibrations of different fuel blends. Their results showed that biodiesel fuel could reduce engine vibration, and hydrogen could reduce the vibration further. Similarly, ethanol-diesel blended fuel has also been investigated for a diesel engine [15], and the RMS and kurtosis were used to scrutinise the performance of the engine.

In other studies, airborne acoustic signals have been used to assess the lubrication quality of the engine. Albarbar et al. [16] studied the effects of lubricating oil based on structure-borne acoustic signals, and found that the amplitude of the spectral components was proportional to the engine speed and load. The RMS values of the signals were found to be influenced by the lubricant conditions.

Some newly developed signal analysis and processing methods have also been used as effective tools for detecting piston scratching faults. In Ref. [15], the short-time Fourier transform (STFT) was developed to characterise various sources of engine vibration. Through an STFT analysis, the authors successfully identified engine knocking cycles when the ethanol concentration in diesel fuel exceeded 8%. Moosavian et al. [17] investigated the vibration signature of a diesel engine under healthy and fault operating conditions, using the fast Fourier transform (FFT) and continuous wavelet transform (CWT) methods to explore the approximate frequency band caused by a piston scratching fault. The results showed that the scratching fault excited the 3–4.7 kHz frequency band [17]. Omar et al. [18] carried out an experimental study in which FFT and STFT were used to compare the vibrations of a liquefied petroleum gas (LPG) dual-fuel engine and a base diesel engine. The results showed that the vibration of the LPG dual-fuel engine was lower than for the diesel engine.

Although the studies described above show that the use of vibration signal is promising in terms of monitoring the tribological behaviours of engine cylinders, there are few studies of the monitoring of two-stroke low-speed marine diesel engines fuelled by HFO, which are vital to prevent the

gradual degradation of cylinder lubrication oil and to avoid any unnecessary wear and corrosion of the cylinder liner.

In this paper, we improve on the findings described above by using a more powerful analysis based on the RMS, FFT, and STFT methods to characterise the engine vibration signals acquired for cylinder lubricating oils with different SAE grades and base numbers, thereby establishing a more accurate and reliable indicator for monitoring the tribological behaviours of the piston ring and cylinder liner of a two-stroke low-speed marine diesel engine. To further verify the diagnostic performance of the vibration signal responses extracted using optimised FFT and STFT spectra, three formulas for cylinder lubricating oils were sampled for elemental analysis after 300 h of steady-state engine operation, and the carbon deposits on the surface of the pistons were compared before and after these 300 h of operation. The main objectives were to explore the effects of different cylinder lubricating oils on the wear to the engine cylinder, and to explore the vibration characteristics of a two-stroke low-speed marine diesel engine fuelled by HFO.

MATERIALS AND METHODS

EXPERIMENTAL SETUP AND DATA ACQUISITION

The experiments were performed on a two-stroke low-speed marine diesel engine, manufactured by MAN B&W corporation, which was installed in the laboratory of Shanghai Maritime University (SMU), China. This type of low-speed diesel engine is widely used in large ocean-going vessels, and is a typical example of such an engine. The engine was fuelled with low-sulphur-content heavy fuel oil (0.5% S) during the experiments. The main technical specifications of this low-speed engine are shown in Table 1.

Tab. 1. Technical specifications of the engine used in the experiments

Item/parameter	Details
Brand	MAN B&W
Model	6S35ME-B9
Engine type	6-cylinder, water-cooled, direct injection, crosshead type
Combustion order	1-5-3-4-2-6
Bore & stroke	350 × 1550 mm
Compression ratio	17:1
Displacement	894 L
Rated output power	3750 kW @ 142 rpm
Maximum indicated pressure	180 bar
Valve opening pressure	380 bar

Three different formulas of cylinder lubricating oil (recipes A, B, and C) were prepared and used. These three cylinder oils all contained the same percentages of additives to the base oil, which included compound ester, ester base, amide, phosphate ester, zinc compound additive, etc., but they had different SAE grades and total base numbers (TBNs). The SAE grade represents the viscosity of the oil. The detailed specifications of these lubricating oils are shown in Table 2. It is worth noting that although the viscosity of recipe B is as same as that of recipe C (both are SAE 40), they have different TBNs.

Tab. 2. Specifications of the lubricating oils used for testing

Lubricating oil	SAE grade	TBN
Recipe A	SAE100	TBN 70
Recipe B	SAE 40	TBN 40
Recipe C	SAE 40	TBN 25

Fig. 1 presents a schematic diagram of the experimental setup used for vibration testing, which shows the connections between the accelerometer, proximity sensor, power supply, data acquisition system, load control system, and a laptop computer with a measuring system. A dynamometer was employed to apply the load to the engine via a load control system. The accelerometer was mounted on the engine head, and a proximity sensor was coupled to the crankshaft to measure its angle. The signals from both transducers were transferred to a data acquisition system (INV3062-C2(L)), and the output data cable was connected to the data acquisition system and a laptop computer to transfer the data. Finally, the data were analysed by a measuring system in the laptop computer. The electricity for the data acquisition system was provided by a power supply.

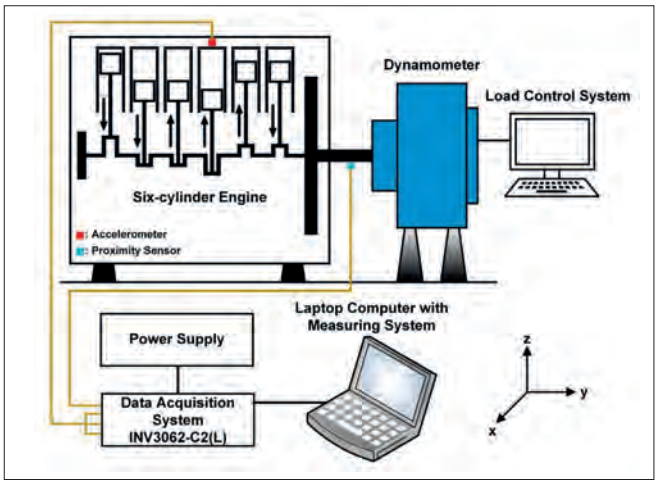

Fig. 1. Schematic diagram of the experimental setup.

The vibration signals were measured with a tri-axial vibration accelerometer (made by Coinv, China). Detailed specifications of the transducers are shown in Table 3. As can be seen from Fig. 1, the accelerometer was mounted on the engine cylinder cover, and the vibrations in three directions (x, y, z) were all acquired by the accelerometer simultaneously. The vibration signals were measured under the same engine load condition for each of the three cylinder lubricating oils. The angle of the engine crankshaft was recorded by the proximity sensor during the vibration measurements. The coordinate system used for both the accelerometer and the engine is shown to the lower right of Fig. 1.

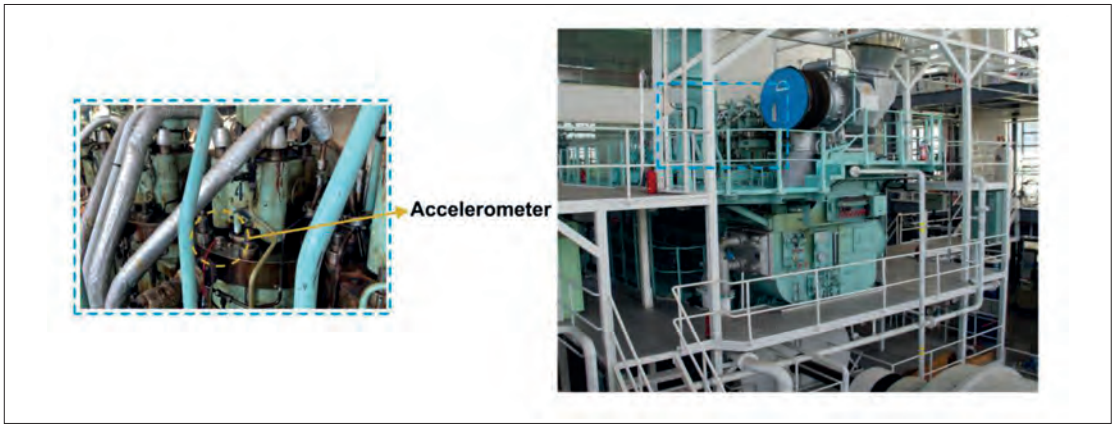

Fig. 2. Installation layout of the experimental equipment.

Tab. 3. Accelerometer specifications

Item/parameter	Details
Type	INV9832-50
Sensitivity	100 mV/g
Measuring range	0.4–12,000 Hz
Weight	12 g
Size	19×19×19 mm^3
Temperature	–50 to 120 °C

The locations at which the vibration sensors were installed are shown in Fig. 2.

In order to approximate the engine operating conditions for the navigation of a real ship, the experiments included three different engine loads (25%, 40%, and 50%). Each sampling was performed after the engine speed had stabilised over 6 h. The data acquisition period was approximately 30 s, and the sampling frequency was 5 kHz for each record; these values of the sampling time and frequency allowed sufficient engine operating cycles to be recorded. The other parameters of the engine, such as its speed, output power, and torque, are shown in Table 4.

Tab. 4. Additional engine parameters

Engine load	Engine speed	Output power	Torque
25%	98 rpm	812.5 kW	91.64 kN·m
40%	105 rpm	1300 kW	116.13 kN·m
50%	113 rpm	1625 kW	136.40 kN·m

ANALYSIS METHODS

In order to compare the differences between the vibration signals in the time domain, the values of the RMS, kurtosis, mean, skewness, standard deviation, and squared deviation of the signals were considered.

For the frequency and time-frequency domain analyses, the FFT and STFT were used. These analyses were all performed using MATLAB (2019 b) and Origin software.

RMS of acceleration signal

The RMS represents the strength of the signal, and is also an expression of the average energy of the signal. The RMS along each axis for all experiments was calculated using Eq. (1) [9]:

$$x_{RMS} = \sqrt{\frac{1}{N}\sum_{i=1}^{N} x_i^2} \tag{1}$$

where x_{RMS} (m/s^2) is the value of the *RMS* for the calculated signal.

To compare the total vibration for each cylinder, the values of RMS_{total} were calculated for three axes (x, y, and z) using Eq. (2) [15]:

$$RMS_{Total} = \sqrt{RMS_x^2 + RMS_y^2 + RMS_z^2} \tag{2}$$

where RMS_{Total} (m/s^2) is the total vibration acceleration, and RMS_x, RMS_y and RMS_z are the *RMS* values for the accelerations along the x, y, and z axes, respectively.

Kurtosis of acceleration signal

The kurtosis is a parameter used to describe the sharpness of a signal distribution. In general, the sharper the signal centroid, the higher the kurtosis. The magnitude of its value can be regarded as the degree to which the signal is abnormal. To analyse the kurtosis, its value was calculated using Eq. (3) [9]:

$$x_{Kurtosis} = \frac{\sum_{i=1}^{N}(x_i - \bar{x})^4}{(N-1)\sigma^4} \tag{3}$$

To compare the total vibration in each cylinder based on the kurtosis, $Kurtosis_{total}$ was derived from the values for the x, y and z axes using Eq. (4) [15]:

$$Kurtosis_{Total} = \sqrt{Kurt_x^2 + Kurt_y^2 + Kurt_z^2} \tag{4}$$

where $Kurtosis_{Total}$ is the total vibration acceleration, and $Kurt_x$, $Kurt_y$ and $Kurt_z$ are the values of the kurtosis for accelerations along the x, y, and z axes, respectively.

Mean of acceleration signals

The mean is the sum of all the data in a set divided by the total number of data points. It is used to reflect the general overall level of data, and can be calculated using Eq. (5) [9]:

$$\bar{x} = \frac{1}{N}\sum_{i=1}^{N} x_i \tag{5}$$

Skewness of acceleration signals

The skewed direction and degree of the signals can be described by the skewness parameter. The skewness value determines whether the signal has a positive, negative, or zero skew (normal distribution), and is calculated by Eq. (6) [9]:

$$x_{Skewness} = \frac{\sum_{i=1}^{N}(x_i - \bar{x})^3}{(N-1)\sigma^3} \tag{6}$$

Standard deviation of acceleration signals

The standard deviation of the arithmetic square root of the squared deviation, which indicates the degree of dispersion between samples of vibration data, is defined by Eq. (7) [10]:

$$\sigma = \sqrt{\frac{\sum_{i=1}^{N}(x_i - \bar{x})^2}{N}} \tag{7}$$

Squared deviation of acceleration signals

The squared deviation of signals represents the degree of fluctuation of the signal around the mean; it can also be understood as the degree of vibration signal shock that exists. It is calculated using Eq. (8):

$$\delta = \frac{1}{N}\sum_{i=1}^{N}(x_i - \bar{x})^2 \tag{8}$$

Fast Fourier transform

The feature parameters mentioned above are quantitative assessments of the time domain of signals, whereas an analysis of the frequency domain of the signal is also required. The FFT can be used to convert a signal from the time domain to the frequency domain, so that the frequency-domain content of the signal can be obtained. The FFT is defined as shown in Eq. (9) [15]:

$$X(k) = \sum_{j=1}^{n} X(j) W_n^{(j-1)(k-1)} \tag{9}$$

where n is the length of signal X, and $W_n = e^{(-2\pi i)/n}$.

Short-time Fourier transform

In the STFT, a signal is split into multiple segments using a window function (in our analysis, the Hamming window function was used). The FFT is then applied to calculate each segment of the signal, and the spectrograms obtained from the FFT are arranged along the time axis, to obtain the time-frequency diagram. Hence, one of the advantages of the STFT over the FFT is that the time and frequency information can both be retained simultaneously, as the time information is lost when the FFT is used. Another advantage is that the STFT can be applied to non-stationary signals, which is not possible for the FFT. The formula for the STFT is given in Eq. (10) [17]:

$$STIF(\tau, f) = \int_{-\infty}^{+\infty} x(t)h(t-\tau)e^{-j2\pi ft} \tag{10}$$

where h is a window function. f and τ denote the frequency and time variables, respectively.

However, the STFT also has certain limitations, as the size of the window cannot change with frequency. Thus, the time and frequency resolution cannot be optimised at the same time in the STFT. The shorter the window, the more obvious the time-domain features become, and the frequency-domain features become more insignificant; conversely, the longer the window, the clearer the frequency-domain features and the more indistinct the time features.

RESULTS AND DISCUSSION

The objectives of this study were to compare the effects of three different lubricating oils on a two-stroke low-speed marine diesel engine, and to explore the vibration of the engine under low to medium load conditions. The results of the experimental study are therefore presented in four sections relating to the time domain, the frequency domain, a time-frequency domain analysis of the vibration signal, and an elemental spectra analysis.

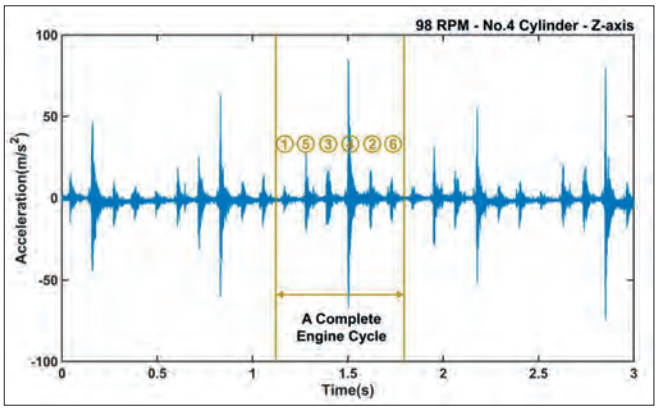

Fig. 3. A complete engine cycle in the time domain

TIME DOMAIN ANALYSIS OF VIBRATION SIGNALS

The lubricating oil not only provides lubrication and reduces friction between the cylinder and piston ring, but also participates in the combustion process. The vibration of an IC engine mainly arises from the gas force generated by the combustion in the cylinders, and a prior study [19] was conducted to explore the in-cylinder combustion process of a low-speed engine using the CFD method. The usage of different lubricating oils is also a crucial factor affecting the vibration in the engine. To investigate the detailed information for the time domain, we consider the z 3 s segment of the signal in Fig. 3, where a complete engine cycle is marked by red lines. This signal represents the conditions with lubricating oil recipe B, at an engine speed of 98 rpm under a load of 25%, along the z-axis. As shown in the figure, the firing order of the cylinders is 1-5-3-4-2-6. The acceleration of the vibration signal in cylinder 4 has the maximum value, while that of cylinder 1 shows the minimum. The reason for this is that the accelerometer was mounted on the head of cylinder 4, whereas cylinder 1 was farthest from the accelerometer. The acceleration values for the other cylinders decrease with increasing distance from cylinder 4. The recording period for the vibration signal was 30.1056 s, containing 150,528 samples. Hence, for an engine speed of 98 rpm, it can be calculated that the duration of

a complete cycle under the 25% load condition is approximately 0.6122 s, containing 3,061 samples. Similarly, from the speeds in Table 4, we can calculate the time for a complete cycle under the 40% load condition as 0.5714 s, and that under the 50% load condition as 0.5310 s.

Before carrying out a frequency domain signal analysis, we calculated the time domain feature parameters (RMS, RMS_{Total}, kurtosis, $Kurtosis_{Total}$, mean, skewness, standard deviation, and squared deviation) for the vibration signals for the three recipes of lubricating oil for 15 complete engine cycles at loads of 25%, 40%, and 50%. Figs. 4 and 5 display scattergrams of the calculated results, showing 15 data points for each recipe under each load condition.

Firstly, the value of the RMS for each axis was calculated using Eq. (1) and the calculation results for the z-axis are shown in Fig. 4a. It can be clearly seen that the RMS values for recipe B are low for all three load conditions, and the data points for this recipe are relatively concentrated. This indicates that the marine diesel engine experiences low vibration along the z-axis under low to medium load when lubricated with lubricating oil based on recipe B. It also suggests that the medium-level TBN of cylinder oil is better matched to its low-sulphur property and gives better engine performance. Recipe A also gave low RMS values under the 25% and 40% load conditions, in a similar way to recipe B. However, under the 50% load condition, there was an increase in some of the RMS values compared to the previous low load conditions. For recipe C, the RMS values show fluctuations under each of the three loads, meaning that TBN values that are too high or too low are not conducive to stable engine vibration.

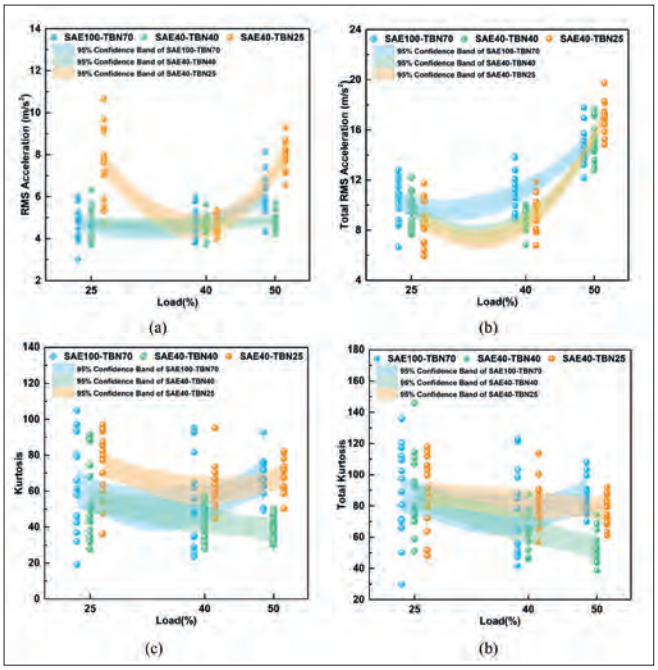

Fig. 4. Plots of feature parameter values for three engine loads for three recipes of lubricating oil: (a) RMS; (b) ; (c) kurtosis; (d) .

The RMS values for each recipe of lubricating oil are low under the 40% load condition. The reason for this is related to the characteristics of this diesel engine, as different lubricating oils have little effect on the intensity of engine vibrations under a 40% load. To enable a comparison of the total vibration of the diesel engine, the RMS_{Total} of the vibration signal was calculated for the *x*, *y*, and *z* vibrations using Eq. (2). There are clear similarities in Fig. 4(b) between the data for the RMS and RMS_{Total} for recipe *B* under the 25% and 40% load conditions. However, under a load of 50%, an increase in RMS_{Total} is observed for recipes *A*, *B* and *C* compared to the RMS. This suggests that the vibrations along the other two axes are increased under the 50% load condition due to the centrifugal inertia force.

Figs. 4(c) and 4(d) show a high degree of similarity between the data point distributions of the kurtosis and $Kurtosis_{Total}$. Under a 25% load, the data points are scattered, whereas when the load is increased, the data points become more concentrated. This indicates that the vibration signal for this marine diesel engine is comparatively sharp under low load conditions, but shows improvement as the load increases. We can also see that the data points for recipe *B* are concentrated at lower values compared to the other two recipes of lubricating oil. The results for the kurtosis showed a trend that was consistent with the results for the RMS. Thus, recipe *B* for the lubricating oil gives better vibration performance for this diesel engine.

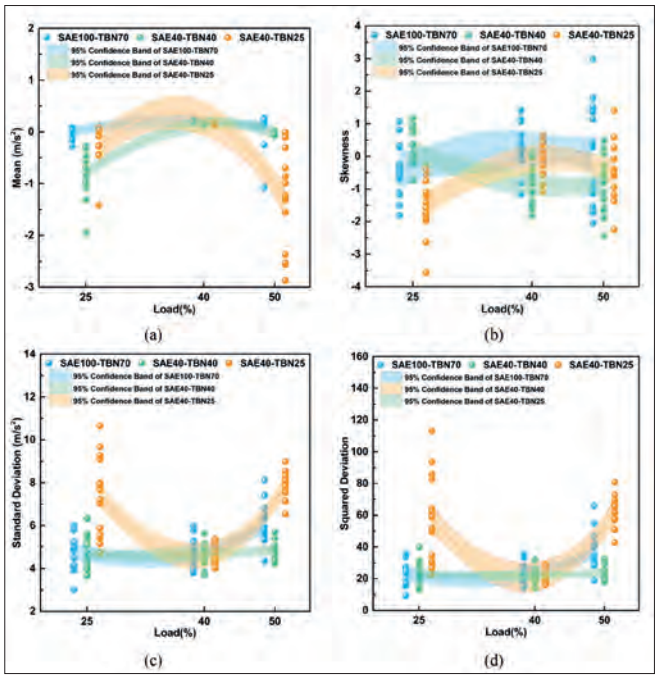

Fig. 5. Plots of feature parameter values for three engine loads for three recipes of lubricating oil: (a) mean; (b) skewness; (c) standard deviation; (d) squared deviation.

Fig. 5 shows the values of the mean, skewness, standard deviation, and squared deviation. For each of the three loads, the mean values for recipe *A* are almost all near zero, while the mean values for recipe *B* remain near zero only for the 40% and 50% load conditions. It is not hard to observe from Fig. 5(a) that the mean values of all three lubricating oils are relatively steady and remain near zero under the 40% load condition. Fig. 5(b) shows that under the 40% and 50% load conditions, recipe *B* has low values for the RMS, kurtosis, and mean, whereas its skewness values are almost all negative. In contrast, the data points for recipe *A* are uniformly distributed on both sides of zero, and do not vary greatly between the load conditions. Furthermore,

it is clear that the data points are most concentrated under the 40% load condition for all three recipes of lubricating oil. In Figs. 5(c) and 5(d), the standard deviation data are fairly close to those of the RMS, and both have almost identical scatter distributions. Meanwhile, the scattergram distribution of the squared deviation is also in accordance with both of the above, despite the different values.

FREQUENCY AND TIME-FREQUENCY DOMAIN ANALYSES OF VIBRATION SIGNALS

In order to further analyse the effects of each oil recipe on the vibration of this two-stroke low-speed diesel engine, the vibration signals along the z-axis under three load conditions were transformed using FFT. Ten consecutive working cycles for each treatment condition were considered for the FFT analysis.

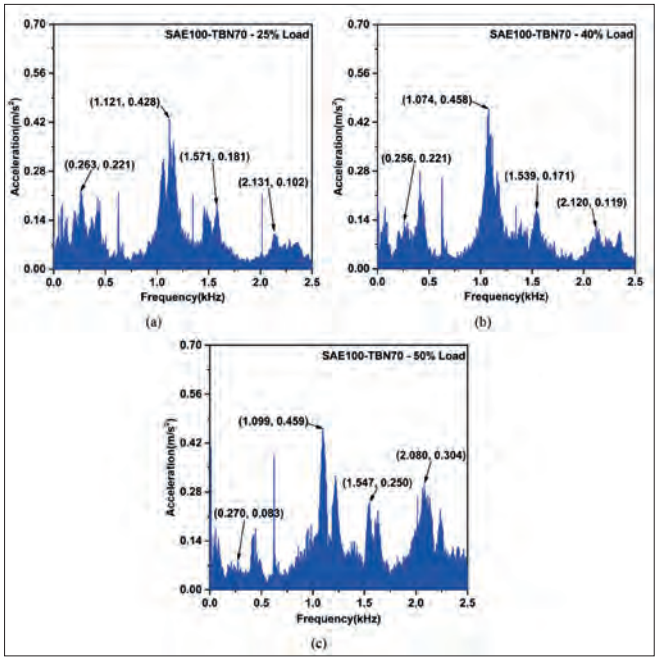

Fig. 6. FFT spectra for recipe A under three typical engine loads: (a) 25%, (b) 40%, (c) 50%.

Figs. 6–8 show FFT spectra for vibration signals under three different engine loads for the three recipes of lubricating oil. It can be observed that the vibration signatures of the diesel engine change when different cylinder lubricating oils are used, from Fig. 6 to Fig. 8. The changed frequency domain of 0–2.5 kHz can be divided into four subdomains: 0.12–0.38 kHz, 0.75–1.3 kHz, 1.3–1.75 kHz, and 1.9–2.5 kHz. In the range 0.12–0.38 kHz, which is the low-frequency region of engine vibration, the accelerations all decrease to varying extents for all three lubricating oils as the load increases, and especially their maximum values. Due to its high viscosity and alkaline nature, the decrease in the maximum value for recipe *A* at a higher load is greater than that for recipes *B* and C, with a decline of 60.2%. The maximum values for recipes *B* and *C* are fairly similar, as they have the same SAE 40 grade. It is known that the low-frequency components of vibration are the main contributors to noise and discomfort for human beings around an engine [18]. It can be seen from the results in Figs. 6–8 that the low-frequency vibration range of this engine shows a decreasing trend as the load increases, which is beneficial to the life of the engine and the comfort of the crew and passengers on board.

The range 0.75–1.3 kHz contains the dominant frequencies of the engine, which are induced by the shock generated by the combustion pressure. Our results show that there are no significant changes in the maximum value in this subdomain for recipes *A* and *C*. For example, the maximum values of recipe *C* in this range are close to 0.330 m/s^2. However, the maximum values of recipe B show a certain degree of reduction, with a decline of 27.7%. This finding indicates that although lowering the alkalinity to a moderate level facilitates lightening the intensity of the engine combustion, a TBN level that is too low does not significantly improve the vibration from engine combustion.

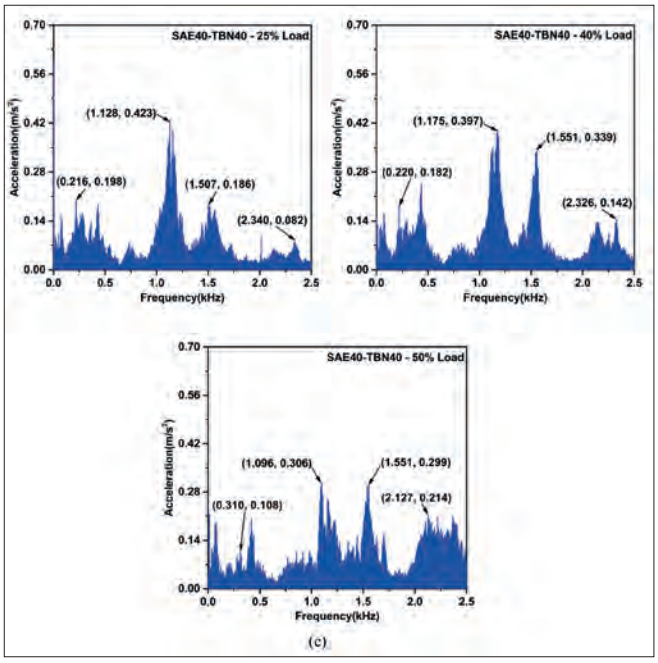

Fig. 7. FFT spectra for recipe B under three typical engine loads: (a) 25%, (b) 40%, (c) 50%.

In the range 1.3–1.75 kHz, all three recipes for the lubricating oil show different trends with increasing load. However, under the 50% load condition, their maximum values are all at a relatively low level of below 0.34 m/s^2. The changes in the maximum values for recipes A and B are similar in the high-frequency subdomain (1.9–2.5 kHz), as both increase with rising loads. The increase in the maximum value for recipe *A* is 198%, and for recipe *B* it is 161%. It is notable that the maximum value under 25% load is 0.426 m/s^2 for recipe *C*, which is higher than for its principal frequency domain. However, under the 40% load condition, the maximum value is only 0.1 m/s^2, while the value is 0.352 m/s^2 under the 50% load condition. We conclude that under low to medium loads, using lubricating oil with recipe *C* causes high-frequency vibration fluctuations in the engine. This also provides some evidence that a TBN level that is too low may affect the detergency between the piston and liner.

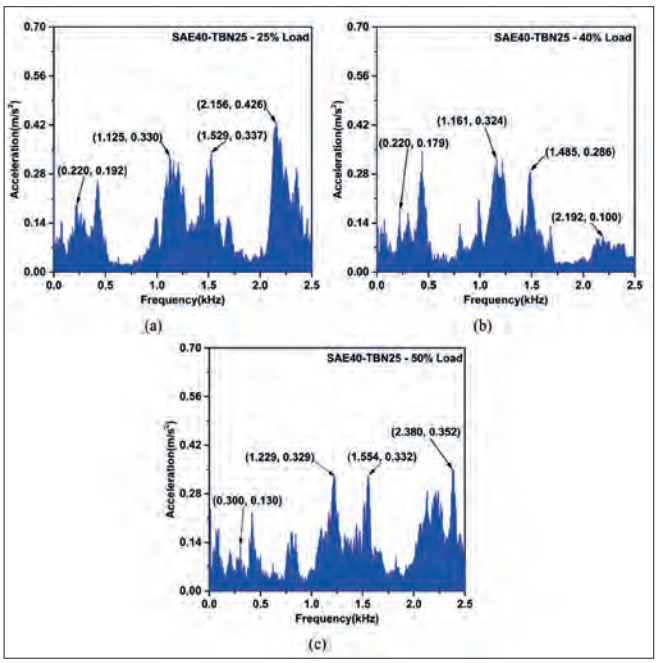

Fig. 8. FFT spectra for recipe C under three typical engine loads: (a) 25%, (b) 40%, (c) 50%.

Furthermore, from the time-domain parameters described above, it can be seen that the vibration data for this engine with these three lubricating oils are relatively centralised under a 40% load, which implies good stability of the engine. In order to further explore the effects of the three oil recipes on the engine vibration characteristics, the STFT method was applied to analyse only the vibration signals under the 40% load condition. Unlike the FFT method, the STFT method involves time information, meaning that the differences between various engine cycles can be observed in the STFT spectra. The signals analysed for each of the above segments all had a length of 5.714 s, and contained 10 consecutive engine cycles.

In Fig. 9, each STFT diagram contains 10 obvious spectrum peaks, representing the 10 engine cycles. In each cycle, several lower peaks can be seen, indicating the vibration of the remaining cylinders; the amplitude for the cylinder on which the tri-axis vibration sensor was mounted on is the largest, and the amplitudes for the other cylinders decrease towards both sides of the engine. The STFT method can be used to analyse engine vibration caused by combustion and friction. This approach is an excellent visualisation tool for monitoring the condition of diesel engines, and can easily provide information about engine vibration and combustion. Since combustion occurs inside the cylinder, it cannot be observed readily. Hence, the state of combustion which is non-visualized can be observed using the STFT method.

As can be seen from Fig. 9a, at 40% engine load, the maximum vibration amplitude of the low-speed marine engine is around 1.5 kHz for all three oils, where the vibration is mainly caused by combustion. Recipe *A* shows three consecutive periods of unusually high amplitude in the frequency band 1.3–1.75 kHz; there are also two continuous engine cycles where the amplitude is extremely low. In Fig. 9(c), the peak of each cycle in the 1.9–2.5 kHz range for recipe *C* is comparable to the values for recipes *A* and *B*, but the vibration of the other cylinders is much lower than for recipes *A* and *B*. What can be clearly seen in the 10 cycles for recipe *B* is better stability in all four subdomains. This further corroborates the findings for the time domain, and indicates that recipe *B* has the best vibration characteristics of the three lubricating oils under 40% load conditions.

LINER WEAR ANALYSIS

The carbon deposits on the surface of each piston were compared before and after 300 h of steady-state engine operation. These deposits covered the surface of each piston with a similar thickness, and were mainly composed of the combustion products from the HFO and cylinder lubricating oils as well as piston-cylinder frictional wear particles, of which the major elements were C, O, S, Fe, and Al.

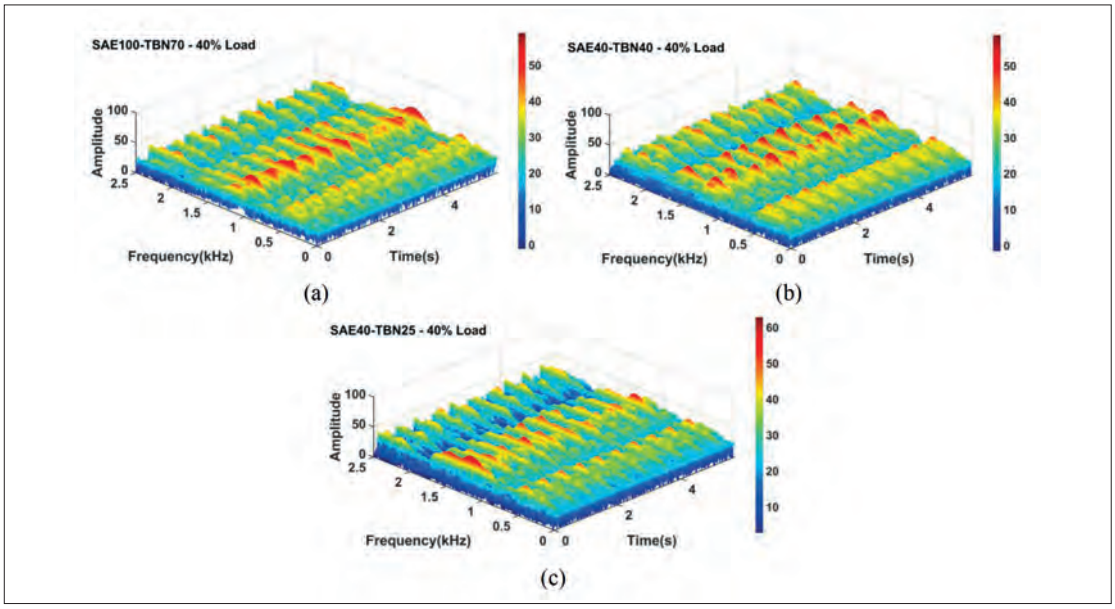

Fig. 9. STFT diagrams for lubricating oils under 40% load: (a) recipe A; (b) recipe B; (c) recipe C.

In order to study the main components of the frictional wear particles, the elements in the lubricating oil were measured through an oil analysis. Several typical elements were selected to compare their contents for evaluation. The cylinder of the marine diesel engine was mainly made of iron-carbon alloy, meaning that Fe was the main metallic element. Al and Si were the main components of the piston, while Mn, Cu, and Ni were also contained in the piston material. Since the three lubricating oils have the same additive ratio but different formulas, they varied in terms of the content of each metallic material before service. We therefore calculated the difference value (D-value) for each major element before and after service. From Fig. 10, it can be seen that the D-values of Fe are 75.2×10^{-6} for recipe B, 80×10^{-6} for recipe *A*, and 88.2×10^{-6} for recipe *C*, meaning that the D-value for recipe *B* is the lowest. For the other five elements, the D-values are also the lowest for recipe *B*, followed by recipe *A* and then recipe *C*. This indicates that recipe *B* has the best anti-wear performance of the three types of oil.

Recipe *C* has the same SAE grade as recipe *B* but a lower TBN value, meaning that its alkali level is too low to completely neutralise the acids of combustion; the un-neutralised acid will attack the piston liners, resulting in corrosive wear and more wear debris during the operation of the pistons. Thus, a cylinder lubricating oil with medium alkali values provides better anti-wear properties than one with a low alkali value. Recipe *A* has a somewhat higher D-value than recipe *B*. One reason for this is that its excess alkali is in the form of inorganic calcium carbonate that cannot be burned, causing hard deposits and three-body abrasive wear between the piston and cylinder. The high viscosity of recipe *A* will also increase the friction loss of the engine, and may increase the wear of the piston-cylinder assembly to a certain extent. In brief, a cylinder lubricating oil with a medium level of viscosity and a medium alkali value has the best anti-wear properties.

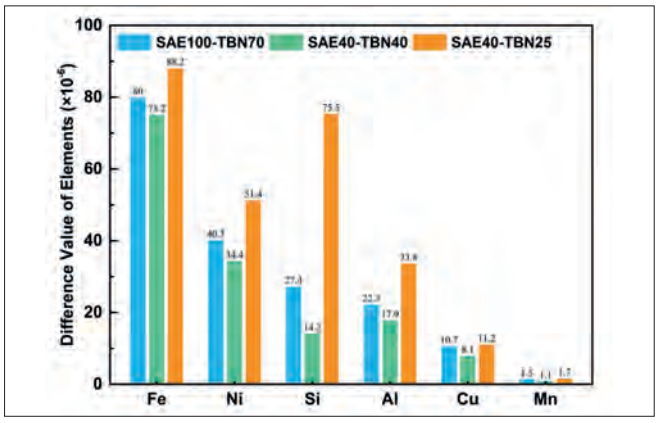

Fig. 10. Difference values for each major element before and after service.

CONCLUSION

In this experimental study, the vibration signals for three different cylinder lubricating oils were measured using a six-cylinder low-speed marine diesel engine (MAN B&W 6S35ME-B9). The main objectives were to analyse the effects of the lubricating oils on engine vibration, in order to select the optimum lubricating oil to reduce wear, and to investigate the vibration characteristics of the low-speed engine under typical load conditions. A triaxial vibration transducer was placed at planned locations. The vibration signals obtained in the experiments were analysed using various time domain characteristics, FFT and STFT. The metallic elements in the cylinder lubricating oils were also measured via an oil analysis before and after operation. The conclusions from the experiment can be summarised as follows.

The vibration characteristics of the two-stroke, low-speed marine diesel engine operating on heavy fuel oil were first investigated, and it was found that the characteristic time-domain parameters of the vibration signal were relatively stable at low engine loads, due to the reduced friction frequency. The alkalinity and viscosity characteristics of the cylinder lubricant had the least effect on the engine vibration under a 40% load. The influence of the cylinder lubricant on engine vibration gradually increased as the load increased.

Under typical ship propulsion loads, recipe *B* was found to have the most concentrated and stable data distributions for RMS, kurtosis, mean, skewness, standard deviation, and squared deviation of the three lubricating oils. This indicates that the medium level alkaline value and medium level viscosity of the cylinder oil are more suitable for low-sulphur heavy oil and cause less wear of cylinder liners and less vibration of the engine.

Real-time FFT and STFT methods were successfully used for non-invasive monitoring of the cylinder liner wear of a marine engine. The sub-ranges of the FFT graphs also show that moderately alkaline cylinder oils improve engine smoothness, while excessively low alkaline levels can worsen vibration in the engine combustion chamber. The STFT method was used as a new way to visually analyse the cylinder under its operating conditions in terms of time and frequency, and the results agreed well with those of a time domain analysis and offline elemental analysis.

This study has presented the results of a vibration data analysis of a two-stroke low-speed marine diesel engine in healthy condition under low to medium operating conditions, which can serve as a data reference for future fault monitoring. Fault diagnosis of a two-stroke low-speed marine diesel engine will be explored in our future work.

AUTHOR CONTRIBUTIONS

Gang Wu: Conceptualization, Methodology, Investigation, Writing - original draft & editing, Funding acquisition. Guodong Jiang: Investigation, Experimentation, Data curation, Writing - original draft & editing. Changsheng Chen: Conceptualization, Methodology. Guohe Jiang: Writing - review. Xigang Pu: Experimentation. Biwen Chen: Writing - review.

ACKNOWLEDGEMENT

The authors disclose receipt of the following financial support for the research, authorship, or publication of this article: This work was supported by the Science & Technology Commission

of Shanghai Municipality and Shanghai Engineering Research Center of Ship Intelligent Maintenance and Energy Efficiency under Grant 20DZ2252300.

CONFLICTS OF INTEREST

The author(s) declare no potential conflicts of interest with respect to the research, authorship, and/or publication of this article.

REFERENCES

1. A. M. K. P. Taylor, „Science review of internal combustion engines," *Energ. Policy*, vol. 36, no. 12, pp. 4657-4667, 2008, https://doi.org/10.1016/j.enpol.2008.09.001.

2. M. Yang et al., „Matching method of electric turbo compound for two-stroke low-speed marine diesel engine," *Appl. Therm. Eng.*, vol. 158, 2019, https://doi.org/10.1016/j.applthermaleng.2019.113752.

3. J. Kałużny et al., „Reducing friction and engine vibrations with trace amounts of carbon nanotubes in the lubricating oil," *Tribol. Int.*, vol. 151, 2020, https://doi.org/10.1016/j.triboint.2020.106484.

4. W. Li, Y. Guo, X. Lu, X. Ma, T. He, and D. Zou, „Tribological effect of piston ring pack on the crankshaft torsional vibration of diesel engine," *Int. J. Engine Res.*, vol. 16, no. 7, pp. 908-921, 2014, https://doi.org/10.1177/1468087414556134.

5. Ö. Böyükdipi, G. Tüccar, and H. S. Soyhan, „Experimental investigation and artificial neural networks (ANNs) based prediction of engine vibration of a diesel engine fueled with sunflower biodiesel – NH3 mixtures," *Fuel*, vol. 304, 2021, https://doi.org/10.1016/j.fuel.2021.121462.

6. K. Çelebi, E. Uludamar, and M. Özcanlı, „Evaluation of fuel consumption and vibration characteristic of a compression ignition engine fuelled with high viscosity biodiesel and hydrogen addition," *Int. J. Hydrogen Energ.*, vol. 42, no. 36, pp. 23379-23388, 2017, https://doi.org/10.1016/j.ijhydene.2017.02.066.

7. K. Çelebi, E. Uludamar, E. Tosun, Ş. Yıldızhan, K. Aydın, and M. Özcanlı, „Experimental and artificial neural network approach of noise and vibration characteristic of an unmodified diesel engine fuelled with conventional diesel, and biodiesel blends with natural gas addition," *Fuel*, vol. 197, pp. 159-173, 2017, https://doi.org/10.1016/j.fuel.2017.01.113.

8. G. Chiatti, O. Chiavola, and F. Palmieri, „Vibration and acoustic characteristics of a city-car engine fueled with biodiesel blends," *Appl. Energ.*, vol. 185, pp. 664-670, 2017, https://doi.org/10.1016/j.apenergy.2016.10.119.

9. A. Moosavian, G. Najafi, B. Ghobadian, M. Mirsalim, S. M. Jafari, and P. Sharghi, „Piston scuffing fault and its identification in an IC engine by vibration analysis," *Appl. Acoust.*, vol. 102, pp. 40-48, 2016, https://doi.org/10.1016/j.apacoust.2015.09.002.

10. S. M. Ramteke, H. Chelladurai, and M. Amarnath, „Diagnosis and classification of diesel engine components faults using time–frequency and machine learning approach," *J. Vib. Eng. Technol.*, vol. 10, no. 1, pp. 175-192, 2021, https://doi.org/10.1007/s42417-021-00370-2.

11. E. G. Giakoumis, „Lubricating oil effects on the transient performance of a turbocharged diesel engine," *Energy*, vol. 35, no. 2, pp. 864-873, 2010, https://doi.org/10.1016/j.energy.2009.08.009.

12. A. Taghizadeh-Alisaraei, B. Ghobadian, T. Tavakoli-Hashjin, and S. S. Mohtasebi, „Vibration analysis of a diesel engine using biodiesel and petrodiesel fuel blends," *Fuel*, vol. 102, pp. 414-422, 2012, https://doi.org/10.1016/j.fuel.2012.06.109.

13. K. Nantha Gopal and R. Thundil Karuppa Raj, „Effect of pongamia oil methyl ester–diesel blend on lubricating oil degradation of di compression ignition engine," Fuel, vol. 165, pp. 105-114, 2016, https://doi.org/10.1016/j.fuel.2015.10.031.

14. A. Çalık, „Determination of vibration characteristics of a compression ignition engine operated by hydrogen enriched diesel and biodiesel fuels," *Fuel*, vol. 230, pp. 355-358, 2018, https://doi.org/10.1016/j.fuel.2018.05.053.

15. A. Taghizadeh-Alisaraei and A. Rezaei-Asl, „The effect of added ethanol to diesel fuel on performance, vibration, combustion and knocking of a CI engine," *Fuel*, vol. 185, pp. 718-733, 2016, https://doi.org/10.1016/j.fuel.2016.08.041.

16. A. Albarbar, F. Gu, A. Ball, and A. Starr, „Internal combustion engine lubricating oil condition monitoring based on vibro-acoustic measurements," *Insight*, vol. 49, no. 12, pp. 715-718, 2007, https://doi.org/10.1784/insi.2007.49.12.715.

17. A. Moosavian, G. Najafi, B. Ghobadian, and M. Mirsalim, „The effect of piston scratching fault on the vibration behavior of an IC engine," *Appl. Acoust.*, vol. 126, pp. 91-100, 2017, https://doi.org/10.1016/j.apacoust.2017.05.017.

18. F. K. Omar, M. Y. E. Selim, and S. A. Emam, „Time and frequency analyses of dual-fuel engine block vibration," *Fuel*, vol. 203, pp. 884-893, 2017, https://doi.org/10.1016/j.fuel.2017.05.034.

19. X. Zhou, T. Li, N. Wang, X. Wang, R. Chen, and S. Li, „Pilot diesel-ignited ammonia dual fuel low-speed marine engines: A comparative analysis of ammonia premixed and high-pressure spray combustion modes with CFD simulation," *Renew. Sust. Energ. Rev.*, vol. 173, 2023, https://doi.org/10.1016/j.rser.2022.113108.